



# Kent Academic Repository

Martyna, Agnieszka, Gomez-Llobregat, Jordi, Linden, Martin and Rossman, Jeremy S. (2016) *Curvature Sensing by a Viral Scission Protein*. *Biochemistry*, 55 (25). pp. 3493-3496. ISSN 0006-2960.

## Downloaded from

<https://kar.kent.ac.uk/55989/> The University of Kent's Academic Repository KAR

## The version of record is available from

<https://doi.org/10.1021/acs.biochem.6b00539>

## This document version

Publisher pdf

## DOI for this version

## Licence for this version

CC BY (Attribution)

## Additional information

## Versions of research works

### Versions of Record

If this version is the version of record, it is the same as the published version available on the publisher's web site. Cite as the published version.

### Author Accepted Manuscripts

If this document is identified as the Author Accepted Manuscript it is the version after peer review but before type setting, copy editing or publisher branding. Cite as Surname, Initial. (Year) 'Title of article'. To be published in *Title of Journal*, Volume and issue numbers [peer-reviewed accepted version]. Available at: DOI or URL (Accessed: date).

## Enquiries

If you have questions about this document contact [ResearchSupport@kent.ac.uk](mailto:ResearchSupport@kent.ac.uk). Please include the URL of the record in KAR. If you believe that your, or a third party's rights have been compromised through this document please see our [Take Down policy](https://www.kent.ac.uk/guides/kar-the-kent-academic-repository#policies) (available from <https://www.kent.ac.uk/guides/kar-the-kent-academic-repository#policies>).

## Curvature Sensing by a Viral Scission Protein

Agnieszka Martyna,<sup>†</sup> Jordi Gómez-Llobregat,<sup>‡</sup> Martin Lindén,<sup>‡,§</sup> and Jeremy S. Rossman<sup>\*,†</sup>

<sup>†</sup>School of Biosciences, University of Kent, Canterbury, Kent CT2 7NJ, United Kingdom

<sup>‡</sup>Center for Biomembrane Research, Department of Biochemistry and Biophysics, Stockholm University, SE-106 91 Stockholm, Sweden

### Supporting Information

**ABSTRACT:** Membrane scission is the final step in all budding processes wherein a membrane neck is sufficiently constricted so as to allow for fission and the release of the budded particle. For influenza viruses, membrane scission is mediated by an amphipathic helix (AH) domain in the viral M2 protein. While it is known that the M2AH alters membrane curvature, it is not known how the protein is localized to the center neck of budding virions where it would be able to cause membrane scission. Here, we use molecular dynamics simulations on buckled lipid bilayers to show that the M2AH senses membrane curvature and preferentially localizes to regions of high membrane curvature, comparable to that seen at the center neck of budding influenza viruses. These results were then validated using *in vitro* binding assays to show that the M2AH senses membrane curvature by detecting lipid packing defects in the membrane. Our results show that the M2AH senses membrane curvature and suggest that the AH domain may localize the protein at the viral neck where it can then mediate membrane scission and the release of budding viruses.

Influenza virus budding requires a precise stepwise alteration of membrane curvature leading to the formation of a membrane bud that is attached to the host cell plasma membrane through a small membrane neck. Release of the budding virion requires membrane scission, which is mediated by an amphipathic helix (AH) domain in the influenza virus M2 protein.<sup>1</sup> The influenza virus M2 protein is a 97-amino acid homotetrameric protein that contains a membrane proximal AH with an extended cytoplasmic tail.<sup>2–4</sup> Membrane insertion of the M2AH is sufficient to alter membrane curvature and cause budding *in vitro* and *in vivo*.<sup>1,5</sup> However, to mediate membrane scission, the M2AH needs to specifically bind and insert into the membrane at the constricted neck of the budding virus.

Influenza viruses bud from lipid raft domains on the apical plasma membrane of infected cells. This budding localization is thought to be mediated by the intrinsic raft localization of the viral surface proteins, Hemagglutinin and Neuraminidase. Because of the length of its transmembrane domain, the M2 protein preferentially sorts to the bulk plasma membrane domain and is recruited to the periphery of the lipid raft budding domains only through interactions with the viral M1 matrix protein. This interaction places M2 near the constricted neck of the budding virion; however, scission requires more

precise localization that would place the M2AH at the center of the membrane neck. This study investigates the mechanism of M2AH localization and shows that the M2AH senses membrane curvature and is preferentially located at the highly curved center of a constricted membrane neck where subsequent insertion of the AH would be sufficient to cause membrane scission.

The first 16 amino acids of the M2 cytoplasmic tail form a membrane-parallel AH domain that inserts into the membrane (Figure 1).

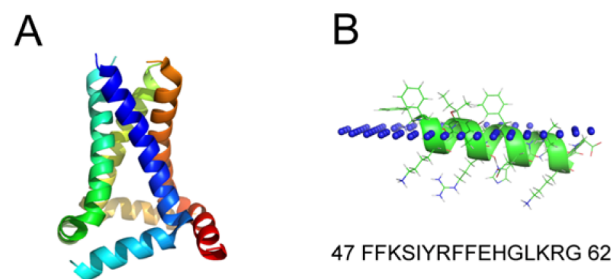


**Figure 1.** Structure of the M2AH. (A) Tetrameric structure of M2 (PDB entry 2L0J). (B) Structure and sequence of the M2AH modeled in the inner leaflet of the lipid bilayer (headgroups depicted as blue dots) generated using E(z)3D.

During virus budding, the M2 protein is recruited to the periphery of the assembly sites.<sup>1</sup> However, to cause membrane scission, M2 needs to localize to the midpoint of the cytoplasmic face of the highly curved budding viral neck, a region that can be topologically depicted as a catenoid (Figure 2A).

Therefore, to determine the specific localization of M2AH, we performed course-grained molecular dynamics (MD) simulations on buckled lipid bilayers.<sup>6</sup> These are planar lipid bilayers that are compressed in one dimension until the bilayers deform. These bilayers show regions of positive, negative, and neutral curvature following the arc length parameter  $S$ , allowing for the determination of any M2AH curvature binding preference (Figure 2B–D).

The simulations show that the M2AH rapidly binds to membranes and inserts at or below the lipid headgroups (Figure 2D). The lipid-bound M2AH then preferentially sorts

Received: May 27, 2016

Revised: June 14, 2016

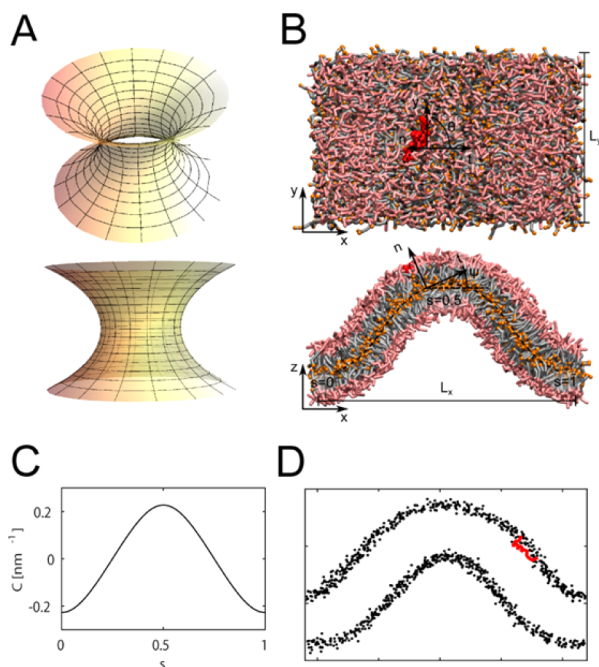


**Figure 2.** MD simulation of M2AH on buckled lipid bilayers. (A) Catenoid structure representative of the neck of a budding virion. (B) Representative top-view (top) and side-view (bottom) snapshots of the MD simulation of the M2AH on lipid bilayers, buckled in the  $L_x$  dimension. Lipid headgroups are colored pink and acyl chains gray. Lipid tail ends are shown as orange spheres, and the M2AH is colored red. Indicated vectors represent the orientation of the M2AH on the bilayer. The side view also shows the Euler buckling profile (blue hashed line) fitted to the bilayer midplane and the corresponding arc length  $S \in [0, 1]$ , which parametrizes the position along the curved membrane midplane (C), with  $s = 0.5$  being the most positively curved position. (D) Side-view snapshot of one location of the M2AH (red) in the buckled bilayer, with the lipid headgroup phosphates shown as black dots.

to regions of high positive membrane curvature (Figure 3A,B and Movies S1 and S2), such as those seen at the narrowest point of the budding neck. While the peptide associated with a range of positively curved membrane domains, the association was the strongest with increased curvature (Figure 3B).

Analysis of the free energy of binding showed that the energy required for binding decreases as the curvature increases (Figure 3C). The binding approached an energy minimum at a radius of curvature comparable to that seen in a 20 nm diameter vesicle; however, absolute quantification would likely require an all-atom simulation. Interestingly, the simulations did not reveal a clear preferred orientation ( $\theta$ ) of the M2AH in the plane of the buckled bilayer surface (Figure 3D). This resembles earlier results for the antimicrobial peptide magainin<sup>6</sup> and suggests that the M2AH may be an isotropic curvature sensor, capable of identifying curved membranes regardless of the orientation of the helix relative to the direction of curvature. Isotropic curvature sensing would be of particular benefit for M2 protein localization as each AH domain in the full length tetrameric protein is oriented at a 90° angle from each other (Figure 1A).

To confirm the MD simulation data, we next performed a liposome binding assay using a fluorescent M2AH peptide. Unilamellar vesicles were made in a range of sizes, which were verified by dynamic light scattering (Figure S1). Vesicles were made without anionic lipids to ensure that charge interactions

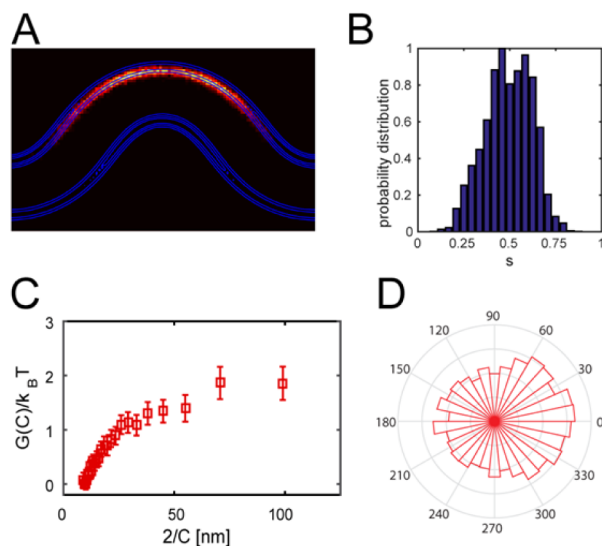


**Figure 3.** M2AH senses membrane curvature. (A) Heat map of the center of mass distribution of the M2AH during the MD simulation, superimposed on the lipid headgroup density (blue level curves). (B) Localization of the M2AH to regions of different curvature during the simulation, shown as a probability distribution and reflecting the arc length parameter  $S$ . (C) Binding free energy at the peptide center of mass on buckled bilayers as a function of the radius of curvature at each given point. (D) Distributions of the in-plane orientation ( $\theta$ ) of single M2AH peptides on bilayers. Because of symmetry in the system, the distributions are periodic (180°). Minor asymmetry arises from statistical fluctuations due to finite sampling, but no additional directional bias is present.

do not mask potential curvature sensing,<sup>7</sup> though this masking was not observed in the simulations. As shown in Figure 4A, the M2AH binds to vesicles that have a diameter between 35 and 3135 nm. The level of binding is slightly reduced for larger vesicles >150 nm in diameter (which possess correspondingly less positive membrane curvature) and significantly enhanced for small vesicles 35 nm in diameter (which have more positive membrane curvature) (Figure 4A).

There is good correlation between the binding results and the MD simulations, both of which show enhancement of binding with increasing membrane curvature (Figures 3B and 4A). In addition, recent bicelle NMR experiments have shown that the M2AH domain can associate with highly curved bicelle edges,<sup>8</sup> further supporting the ability of the M2AH to sense membrane curvature.

Binding results were confirmed using circular dichroism spectroscopy (CD) analysis of peptide secondary structure. The M2AH forms an  $\alpha$ -helix upon membrane binding, and thus, the amount of  $\alpha$ -helix observed in the structure is related to membrane binding activity. CD analysis showed an increasing percentage of  $\alpha$ -helix formation as vesicle size decreased, reaching a maximum when the domain bound to 35 nm vesicles, though in all cases the M2AH was at least 70%  $\alpha$ -helix, indicating that enhanced curvature facilitates but is not necessary for structuring of the AH domain (Figure 4B). Together, these results indicate that the M2AH strongly associates with highly curved membranes, such as would be seen at the neck of budding viruses.

Many AHs, such as those found in N-Bin-Amphiphysin-Rvs (N-BAR) domains and amphipathic lipid packing sensor (ALPS) motifs, are capable of sensing membrane curvature.<sup>7,9</sup> ALPS motifs contain bulky hydrophobic residues on one face of

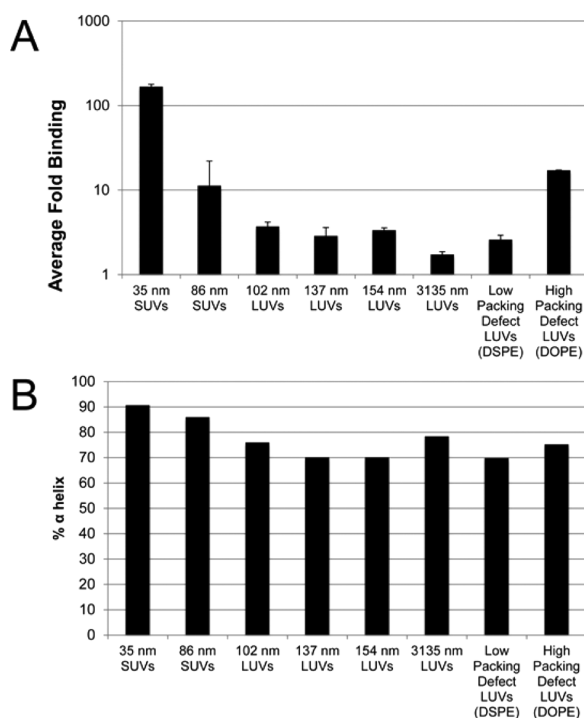


**Figure 4.** M2AH senses membrane curvature *in vitro*. (A) The FITC-labeled M2AH was incubated with POPC vesicles of the indicated size or with 100 nm DOPC:DOPE/DSPE LUVs for 1 h. Fluorescence was determined and is represented as the vesicle-bound fluorescence/background fluorescence. Values are means  $\pm$  the standard deviation of three independent repeats. (B) The M2AH was incubated with indicated vesicles and the secondary structure determined by CD. All measurements are the average of four background-subtracted measurements, shown as %  $\alpha$ -helix using K2D3.

the AH and uncharged residues on the polar face.<sup>7</sup> These motifs sense membrane curvature through insertion of the bulky hydrophobic residue face into lipid packing defects, which are gaps in the lipid bilayer caused by the separation of polar headgroups as a consequence of positive membrane curvature.<sup>7,10</sup> Like the ALPS motif, the hydrophobic face of M2AH also contains multiple bulky hydrophobic residues. To determine whether the M2AH recognizes membrane curvature by sensing lipid packing defects, we evaluated binding of the peptide to LUVs containing fully saturated (DSPE) or monounsaturated (DOPE) lipid tails. DOPE is a cone-shaped lipid that limits how tightly the lipids can pack in a curved bilayer, creating many lipid packing defects. In contrast, DSPE is a cylindrical lipid that allows for tighter packing of the lipid headgroups, resulting in fewer lipid packing defects compared to the number in DOPE bilayers for any given curvature.<sup>11</sup> Thus, a peptide that senses lipid packing defects would be expected to bind more tightly to LUVs containing DOPE than LUVs containing DSPE. We found that the M2AH binds significantly stronger to LUVs with packing defects but shows minimal change in  $\alpha$ -helix content when bound to these LUVs (Figure 4). As DOPE and DSPE have significantly different phase transition temperatures, we confirmed that the observed binding differences were caused by the presence of lipid packing defects and not because of differences in line tension or lipid domain formation. In Figure S2, we see that the M2AH binds comparably to LUVs with a range of different line tensions.<sup>12</sup> Thus, these results suggest that the M2AH identifies

membrane curvature by sensing lipid packing defects, similar to ALPS motifs.

Narrow prestricted membrane necks occur at the junction between a budding influenza virion and the host cell, and infection of cells with influenza viruses that do not express the M2 protein results in the formation of stalled membrane buds that fail to undergo membrane scission.<sup>1</sup> This suggests that M2 is responsible for completing scission at the narrow neck that forms at the site of viral budding. TEM analysis of the stalled buds, formed on the plasma membrane during a  $\Delta$ M2 influenza virus infection, shows a constricted membrane neck with an average radius of curvature at the midpoint of the neck of  $19.84 \pm 7.91$  nm (Figure 5).<sup>1</sup>

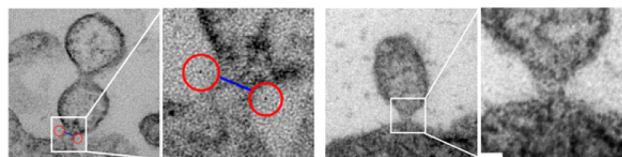


**Figure 5.** Curvature at the neck of budding virions. MDCK cells were infected with A/Udorn/72- $\Delta$ M2 virus for 18 h, fixed, and processed for thin-section TEM.<sup>1</sup> Images were analyzed to determine the average radius of curvature (red circles) at the neck midpoint (blue line) for a minimum of 50 virions. Two representative images and their magnifications are shown. The scale bar represents 20 nm.

These results agree with the results of our liposome binding experiments that showed efficient binding to 35 nm vesicles (possessing a 17.5 nm radius of curvature) and with our molecular dynamics simulations, which showed an increasing level of binding with decreasing vesicle size (Figures 3B and 4A).

This suggests that the M2AH sorts to regions of high membrane curvature similar to that seen at the center of the membrane neck formed during influenza virus budding and is consistent with the observed *in vivo* localization of the M2 protein during virus budding.<sup>1</sup> When the M2 protein is present at the membrane neck during wild-type influenza virus budding, membrane scission is completed and the influenza virion is released.<sup>1</sup>

The M2 protein is thought to localize to the boundary between the viral budding domain and the bulk plasma membrane, which would position the M2 protein near the neck of the budding virus, though it is not clear if this localization is mediated through M2–M1 interactions or because of intrinsic biophysical properties of the full length protein.<sup>13–15</sup> However, to complete membrane scission, M2 needs to act at the midpoint of the constricted neck. Here we show that the M2AH senses membrane curvature (Figure 3B,C) by detecting lipid packing defects occurring at highly curved membranes (Figure 4A). This curvature sensing allows the level of M2AH–membrane binding to increase as the membrane radius of curvature decreases (Figure 3C). This allows for strong binding of the M2AH to membranes with a radius of curvature between 10 and 20 nm, similar to what is seen at the center neck of budding influenza virions (Figure 5).

Thus, M2AH curvature sensing may facilitate placement of the helix at the center of the prestricted membrane neck and could ensure the maintenance of this localization during further constriction. At the neck midpoint, M2AH membrane insertion, and induction of curvature, may be sufficient to cause membrane scission.<sup>1</sup> Thus, the release of influenza viruses likely

requires a specific combination of curvature sensing and curvature induction by the M2AH domain.

## ■ ASSOCIATED CONTENT

### 📄 Supporting Information

The Supporting Information is available free of charge on the ACS Publications website at DOI: [10.1021/acs.biochem.6b00539](https://doi.org/10.1021/acs.biochem.6b00539).

Two figures and experimental methods (PDF)

Movie 1 (MP4)

Movie 2 (MP4)

## ■ AUTHOR INFORMATION

### Corresponding Author

\*School of Biosciences, University of Kent, Canterbury, Kent CT2 7NJ, United Kingdom. E-mail: [j.s.rossman@kent.ac.uk](mailto:j.s.rossman@kent.ac.uk).

### Present Address

§M.L.: Department of Cell and Molecular Biology, Uppsala University, Box 596, 751 24 Uppsala, Sweden.

### Funding

This work was supported by the Medical Research Council (MR/L00870X/1 and MR/L018578/1 to J.S.R.), the European Union Seventh Framework Programme (FP7-PEOPLE-2012-CIG: 333955 to J.S.R.), the Wenner-Gren Foundations, and the Swedish Foundation for Strategic Research via the Center for Biomembrane Research (M.L. and J.G.-L.).

### Notes

The authors declare no competing financial interest.

## ■ ACKNOWLEDGMENTS

Simulations were performed on resources provided by the Swedish National Infrastructure for Computing at the National Supercomputer Centre.

## ■ REFERENCES

- (1) Rossman, J. S., Jing, X., Leser, G. P., and Lamb, R. A. (2010) *Cell* 142, 902–913.
- (2) Rossman, J. S., Jing, X., Leser, G. P., Balannik, V., Pinto, L. H., and Lamb, R. A. (2010) *J. Virol.* 84, 5078–5088.
- (3) Schnell, J. R., and Chou, J. J. (2008) *Nature* 451, 591–595.
- (4) Tian, C., Gao, P. F., Pinto, L. H., Lamb, R. A., and Cross, T. A. (2003) *Protein Sci.* 12, 2597–2605.
- (5) Schmidt, N. W., Mishra, A., Wang, J., DeGrado, W. F., and Wong, G. C. (2013) *J. Am. Chem. Soc.* 135, 13710–13719.
- (6) Gómez-Llobregat, J., Elías-Wolff, F., and Lindén, M. (2016) *Biophys. J.* 110, 197–204.
- (7) Drin, G., and Antonny, B. (2010) *FEBS Lett.* 584, 1840–1847.
- (8) Wang, T., and Hong, M. (2015) *Biochemistry* 54, 2214–2226.
- (9) Bhatia, V. K., Madsen, K. L., Bolinger, P. Y., Kunding, A., Hedegard, P., Gether, U., and Stamou, D. (2009) *EMBO J.* 28, 3303–3314.
- (10) Bigay, J., Casella, J. F., Drin, G., Mesmin, B., and Antonny, B. (2005) *EMBO J.* 24, 2244–2253.
- (11) Nath, S., Dancourt, J., Shteyn, V., Puente, G., Fong, W. M., Nag, S., Bewersdorf, J., Yamamoto, A., Antonny, B., and Melia, T. J. (2014) *Nat. Cell Biol.* 16, 415–424.
- (12) Garcia-Saez, A. J., Chiantia, S., and Schwille, P. (2007) *J. Biol. Chem.* 282, 33537–33544.
- (13) Rossman, J. S., and Lamb, R. A. (2011) *Virology* 411, 229–236.
- (14) Schroeder, C. (2010) *Subcell. Biochem.* 51, 77–108.
- (15) Nayak, D. P., Balogun, R. A., Yamada, H., Zhou, Z. H., and Barman, S. (2009) *Virus Res.* 143, 147–161.